

Measuring Vibration with Piezoelectric Sensors (Part 1)

The Research

By
George Ntanavaras



Several years ago, George Ntanavaras designed a system consisting of the ACH-01 accelerometer and an amplifier with an integrated analog signal processor. Over the years, he has been looking for other possible solutions concerning the vibration measurements. In this article, he describes his research for the design, the construction of such a system, and presents the results and the measurements.

Several years ago in this magazine, I published an article describing the design and operation of a system consisting of the ACH-01 accelerometer and an amplifier with an integrated analog signal processor (see Resources). The cost of the system is very reasonable and proved to be popular among the amateur and professional loudspeaker builders who wanted to investigate vibration issues especially in loudspeaker enclosures. I made the PCB and the front panel of this amplifier available to DIY builders and a lot of amplifiers have been built around the world.

The ACH-01 is a general-purpose, linear single-axis accelerometer housed in a small, rugged, flat package and manufactured by TE Connectivity. According to its datasheet, it is internally buffered for lower output impedance and has a very wide frequency response, typically from 2Hz to 20kHz, with the worst case -3dB response from 5Hz to 10 kHz. It can measure up to approximately 150g and has a high resonance frequency at 35kHz. The linearity is typically 0.1% with a maximum

deviation of 1%. Its output provides an analog voltage directly analogous to the acceleration that it measures. The ACH-01-03 version of the accelerometer is supplied with a shielded cable and a convenient connector.

The amplifier bias the internal junction field effect transistor (JFET) of the ACH with a current source and amplifies its output. It provides three different gain settings to properly adjust the output voltage level and a first-order high-pass filter with three selectable cut-off frequencies. It can be calibrated for each ACH, providing at its output accurate values for the acceleration, the velocity, and the excursion of the object being measured.

A couple of years ago, mostly because I wanted to study the subject in more detail and expand my knowledge, I began looking for other possible solutions concerning the vibration measurements. In this article, I will describe this long-time research for the design and construction of such a system and I will present the results and the measurements I took.

I used the ACH-01 as my reference accelerometer because I didn't have any other accelerometer with better specifications. I have to point out that I didn't have any intention of making a reference system or replacing the ACH accelerometer, which has served me so well for many years now. The system that I will present should be considered as an educational approach to the vibration measurements for amateur builders. The interest here is mainly in the differences existing between the measurements rather than absolute measurements, because the system that I present in this article cannot offer calibrated outputs.

A Simplified View of the Piezoelectric Accelerometer

The piezoelectric accelerometer is widely accepted as the best available sensor for the measurement of vibration. It employs the piezoelectric effect of certain materials to measure dynamic changes in mechanical variables. According to this effect, when a force is applied on the piezoelectric material, a change in its dimensions occurs, which results in the generation of electrical charge.

A simplified version of a piezoelectric accelerometer is shown in **Figure 1**. The active element is the piezoelectric material, which has its bottom side bonded to a rigid base, while a so-called seismic mass is attached to its top side. When the system is vibrating, according to Newton's second law, the force acting on the piezoelectric element is equal to the product of the acceleration and the seismic mass. Due to the piezoelectric effect, a charge output proportional to the applied force is generated. Since the seismic mass is constant, the charge output signal is proportional to the acceleration and is connected to the sensor output via a pair of electrodes.

Sometimes, the mass of the piezoelectric material itself is used as seismic mass, reducing the sensitivity but increasing the resonance frequency of the accelerometer.

Brüel & Kjær has an excellent handbook about the piezoelectric accelerometer. The handbook can be downloaded from the company's website (see Resources) and is highly recommended.

Testing the System

The first thing I had to do was to find a reliable way to test and measure the vibration sensors. I needed a device to produce a defined vibration level, which should be constant through the entire range of interested frequencies. This is

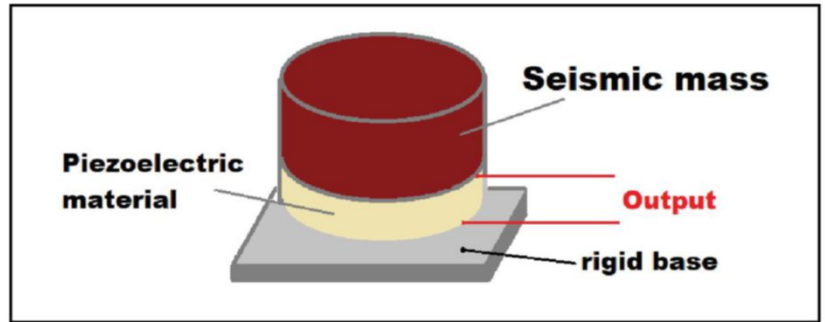


Figure 1: A simplified diagram of an accelerometer

not a problem if you have enough money to buy a mini-size Vibration Shaker or calibration device from any respectable manufacturer.

I decided to look for other solutions with an affordable cost and acceptable results. I had a Peerless driver available from an old subwoofer project, and I began the tests. When I started the project, I was interested in testing only at the low frequencies that could be covered by a subwoofer driver, but then I decided to expand the frequency range.

After a lot of experiments, I ended up with two separate testing systems—one for the frequency range between 5Hz and 300Hz, using a Peerless 830500 XLS 12" driver unit; and a second one for



Photo 1: The Peerless driver with the ACH placed on its cone

the frequency range between 200Hz and 2kHz, using a Visaton BS130 unit.

When a loudspeaker driver is used to test an accelerometer, one very difficult problem is finding an easy way to attach and remove the accelerometer from the cone without causing any damage. The Peerless driver's cone was made from a material to which I could attach the accelerometer and remove it without much difficulty or damage, using double-sided tape. But if it were done several times, after some point, the cone material would start to come off. I solved this by uniformly applying several layers of Loctite 401 instant adhesive to the center of the cone making it stiffer.

The Peerless driver is a very large and heavy unit, and I built a special contraption to support it in the vertical position as shown in **Photo 1**. The driver's frequency response was not very flat at the low frequencies since it was used without any enclosure. I equalized this response using a Linkwitz transform circuit. **Figure 2** shows the electronic diagram of the circuit using an OPA2604 op-amp. To calculate the values of the components, I measured the acceleration of the driver cone by

attaching the ACH sensor to its center. This was found to be similar to a second-order high-pass filter with $f_0=27\text{Hz}$ and $Q_0=0.43$. Then, I set the target response to $f_p=5\text{Hz}$ and $Q_p=0.7$. I used a spreadsheet that I found on the Linkwitz Lab's website (see Resources) to calculate the values of the components.

Photo 2 shows how I built the circuit. The power supply circuit is on the left PCB and the Linkwitz circuit is on the right PCB. The circuit applies a maximum boost of 25.8dB at 3.4Hz to achieve a flat response at the very low frequencies. This requires caution to keep the amplifier voltage that drives the subwoofer at low levels, otherwise the Peerless cone will make very large excursions that could damage it.

Additionally, I used a frequency response compensation file in ARTA software to make a few minor corrections to the response at the frequencies above 150Hz, resulting in an almost flat response as shown in **Figure 3**. The response was taken with the ACH accelerometer attached to the Peerless cone, and it is very flat from 7Hz to 300Hz, where the loudspeaker cone behaves like a rigid piston. The -3dB low-frequency point

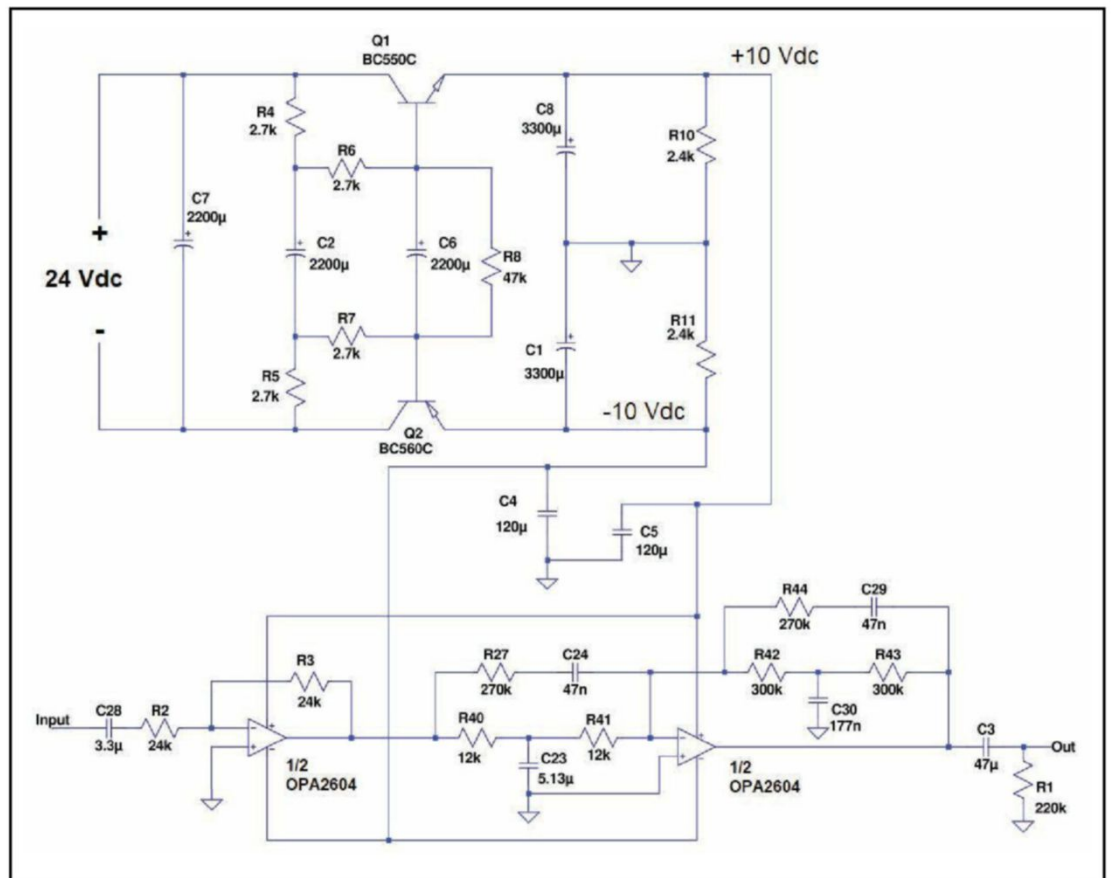


Figure 2: The Linkwitz transform circuit for the Peerless driver

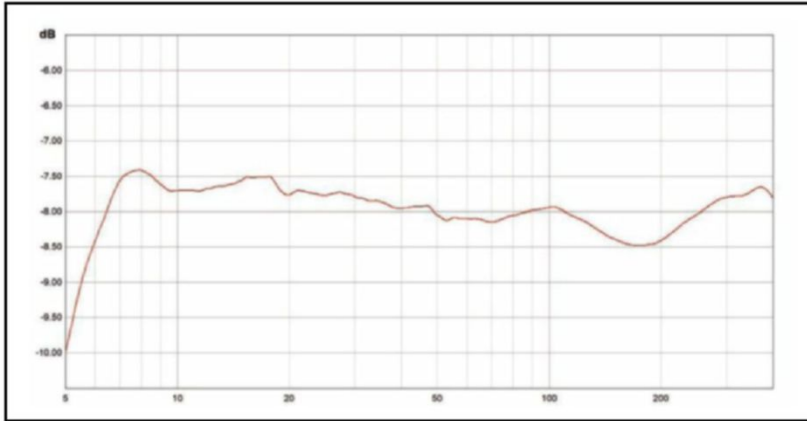


Figure 3: The Peerless cone acceleration after equalization, as measured with ACH



Photo 3: The disassembled Visaton BS-130 unit

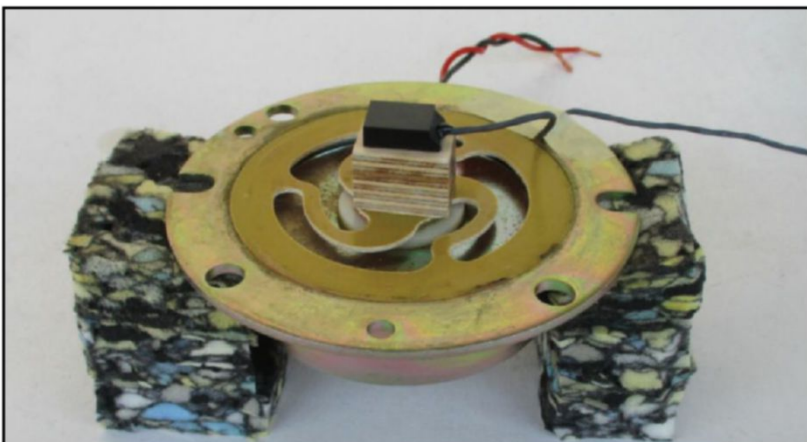


Photo 4: The Visaton BS-130 as modified for the measurements

I additionally placed a small piece of plywood with the dimensions 15mm × 15mm × 25mm to the center of the oscillating plate to attach the sensors using double-sided adhesive tape. The support base for the Bass Shaker is very critical and after some trials I found that the best one was made from a sound absorbing material. The final set-up is shown in **Photo 4**.

The acceleration response of the Bass Shaker with the ACH accelerometer attached (**Figure 4**) is reasonably flat within 0.5dB from 200Hz up to about 2.1kHz. Some minor resonances are shown at 450Hz and above 2.1kHz. Using these two systems, I had the ability to test the sensors with a reliable and repeatable way for the frequency range between 10Hz and 2kHz.

The Murata Shock Sensor

I began my experiments using the Murata shock sensor PKGS-00LDP1-R. This is a high sensitivity, SMD mounted, acceleration sensor with dimensions 6.4mm × 2.8mm × 1.20mm (**Photo 5**).

The sensor consists of a piezo ceramic element, which is stuck between two ceramic substrates. It is designed for hard-disk drive applications, used in personal computers and consumer audio-visual equipment. Its charge sensitivity is 0.84pC/g (±15%) where g is the earth's gravity and has a high nominal resonance frequency at 20kHz. The capacitance of the sensor is 770pF (±30%).

I used the circuit shown in **Figure 5** to amplify the sensor's signal. This circuit is based on the Jensen application note AS098 (see Resources) but I modified it to have unity gain.

I used a JFET in the input and a bipolar transistor buffers the output of the circuit. I built this circuit together with the sensor on a small PCB as shown in Figure 5b. The circuit was supplied by a 12V, very low noise power supply based on a capacitor multiplier.

I attached the PCB to the cone of the Peerless driver and I took an acceleration measurement. The result was very promising. The sensor had a good frequency response, almost similar to that of the ACH-01 sensor. But there was a serious problem—very, very large interference of the 50 Hz mains voltage and its harmonics was present in every measurement. Trying to find a solution, I shielded all around the PCB with an aluminum sheet and I connected it to the ground of the circuit. This gave much better results, but the interference was not totally eliminated.

I decided to continue looking for a better solution that would eliminate this mains interference. Also,

according to Murata’s recommendation, I decided to design and build a charge amplifier circuit to use with the sensor.

The Charge Amplifier

A charge amplifier is a current integrator circuit that produces a voltage output proportional to the electrical charge flowing into its input. It consists of an operational amplifier (op-amp) in an inverting configuration with a feedback impedance that is a capacitor.

A practical circuit is shown in **Figure 6**. The piezoelectric sensor is directly connected to the inverting input. The charge Q produced by the sensor is proportional to the acceleration, and the circuit has an output voltage that is proportional to the acceleration measured by the sensor.

The resistor R_{FB} is needed to properly bias the op-amp.

The “charge gain” G of the amplifier is determined by the feedback capacitance C_{FB} and is given by the following formula:

$$G = \frac{1}{C_{FB}}$$

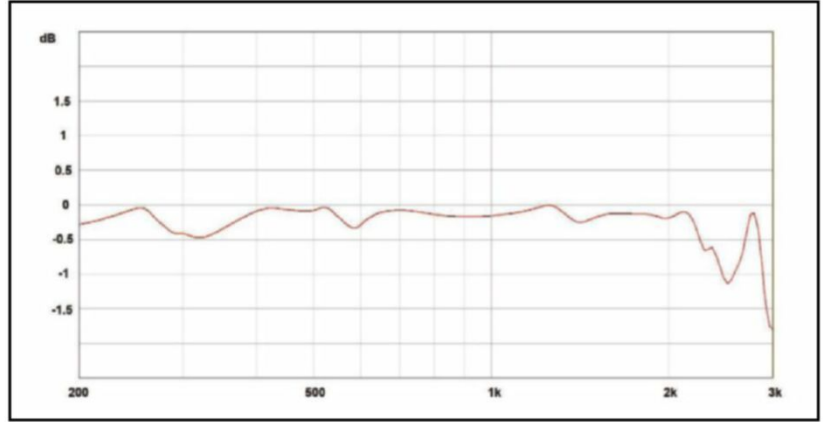


Figure 4: The Visaton Exciter cone acceleration was measured with the ACH accelerameter.



Photo 5: The Murata vibration sensor



NEW
EAR CANAL • IMPEDANCE •
LOW NOISE

BEST TESTING

Experience cutting-edge technology that enables true-to-reality and comprehensive fullband tests for your headphones, headsets and hearables.

HEAD acoustics, Inc. • info@head-acoustics.com • www.head-acoustics.com





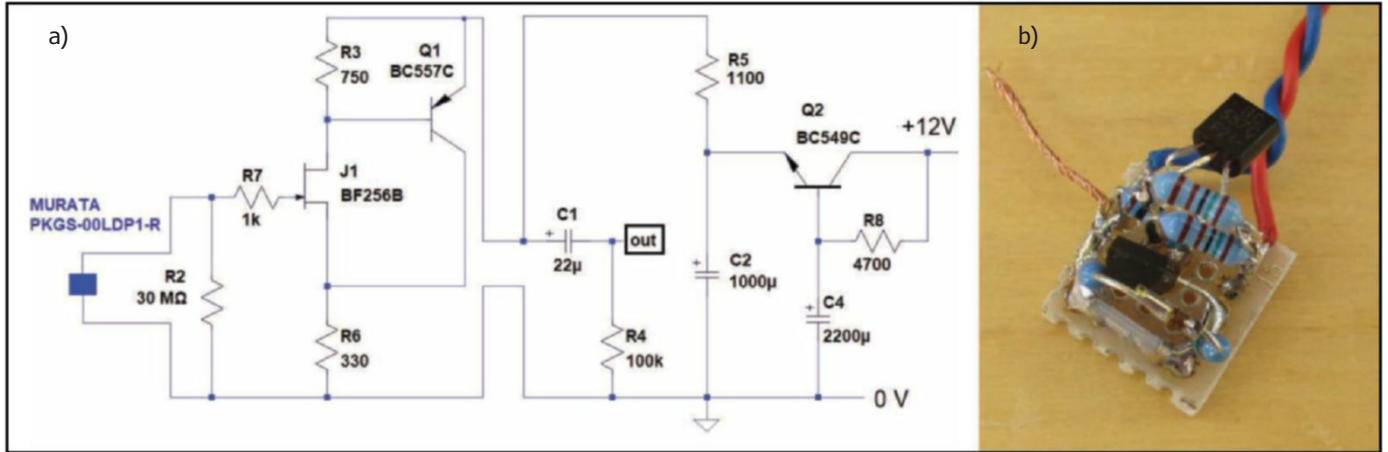
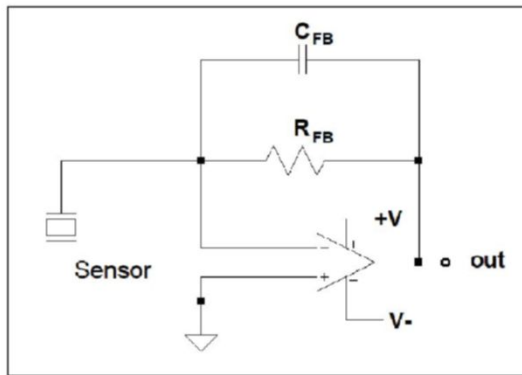


Figure 5: The schematic for the first piezoelectric sensor amplifier attempt (a) and the PCB (b)

Figure 6: A practical circuit for a charge amplifier



The formula indicates that the “charge gain” of the amplifier is independent of the cable capacitance or other input parasitic capacitance around the sensor.

The charge amplifier operates as a high-pass filter with the cut-off frequency F_{HP} given by the following formula:

$$F_{HP} = \frac{1}{(2 \times \pi \times R_{FB} \times C_{FB})}$$

Usually, the capacitance C_{FB} is a few hundred pFs and the resistor R_{FB} should have a very large value, in the order of a few tens of megohms, to achieve a low cut-off frequency. Very high value resistors are not very common, but this can be solved by using several resistors in series.

The input bias current of the op-amp flowing through this high value resistor will produce a large output offset voltage. This could be minimized by choosing an op-amp with very low input bias currents. A field-effect transistor (FET) input amplifier, which usually has an input bias current of a few pA (picoAmperes), will produce a very small offset of a few millivolts, as long as the resistor value is below a few hundred megohms. Then, this output offset can be filtered out very easily with AC coupling to the following stage.

Next Month

In the second part of the article, I will continue with the design and construction of the main piezoelectric sensor and I will present some other sensors that could be used for the vibration system. In the third and final part, I will present the design and construction of the piezoelectric charge amplifier and the measurements that will enable us to evaluate the whole system.

About the Author

George Ntanavaras graduated from the National Technical University, Athens, Greece, in 1986 with a degree in Electronic Engineering. He currently works as a Technical Consultant for Greek electronics companies. He is interested in the design of preamplifiers, active crossovers, power amplifiers, and most loudspeakers. He also enjoys listening to classical music.



Resources

Jensen Transformers, Jensen application note AS098, <https://www.jensen-transformers.com/application-notes>
<https://www.jensen-transformers.com/wp-content/uploads/2014/08/as098.pdf>

Linkwitz Lab, Spreadsheet to calculate the component values of the Linkwitz transform circuit, <http://www.linkwitzlab.com/Linkwitz%20Filter%20Circuits%20Tool%20V4.1.xls>

G. Ntanavaras, “Accelerometer Testing of Loudspeaker Drivers” *audioXpress*, June 2011, <https://www.audioxpress.com/article/Test-your-speakers-performance-with-this-do-it-yourself-measurement-system.html>

M. Serridge and T. R. Licht, *Piezoelectric Accelerometer and Vibration Preamplifier Theory and Application Handbook*, Brüel & Kjær, Revision November 1987, <https://www.bksv.com/media/doc/bb0694.pdf>

Measuring Vibration with Piezoelectric Sensors (Part 2)

Design and Construction

By
George Ntanavaras



In this article series, George Ntanavaras describes his research on measuring vibration using Piezoelectric Sensors. In the second part, he discusses the design of such a system, configurations of the charge amplifiers circuits that he built and tested, and the connections to the piezoelectric sensors. He also presents some additional sensors that could be used for vibration measurements.

Configurations of the Charge Amplifiers

Trying to eliminate the mains interference, I decided to introduce the benefits of the differential amplifier. This type of amplifier is suitable for use in measurement and test equipment since it amplifies the voltage difference between its two inputs by some constant factor and rejects the part of the signal that are common to both inputs.

Figure 1 shows the electronic diagram for four circuits that I tested. All of them, are based on the LMC6482 CMOS operational amplifier (op-amp). It has an ultra-low input current of only 0.02pA and a very high input impedance of 10TΩ. **Photo 1** shows the construction of these circuits on prototype PCBs.

Circuit 3 is a charge amplifier based on only one op-amp U1 with differential inputs. Resistors R5 and R6 provide ESD protection. The capacitors C1, C13 and C2, C12 adjust the gain of the charge amplifier and resistors R1 and R3 provide the bias. The second op-amp U2 provides some additional gain.

Circuit 4 uses two single-ended charge amplifiers around U1 and U2, one for each side of the signal

while a third op-amp U3 transforms the balanced signal to a single-ended signal.

Circuit 5 is the classical differential voltage amplifier using three op-amps. And Circuit 6 uses two similar voltage buffers U1 and U2 for the positive and negative side of the input signal and a low-cost instrumentation amplifier U4 to transform the balanced signal to a single ended signal.

The circuits were supplied by an external 24VDC switched mode power supply followed by a capacitance multiplier circuit to produce a very low noise supply voltage. I thought that the circuits would show different behavior, but all of them measured well and their output noise was almost identical while the mains interference was reduced. I decided to use the Circuit 3, mostly because of its simplicity.

Sensor Arrangements

I also tested different sensor arrangements trying to increase the output level and possibly find a layout that will reduce the mains interference.

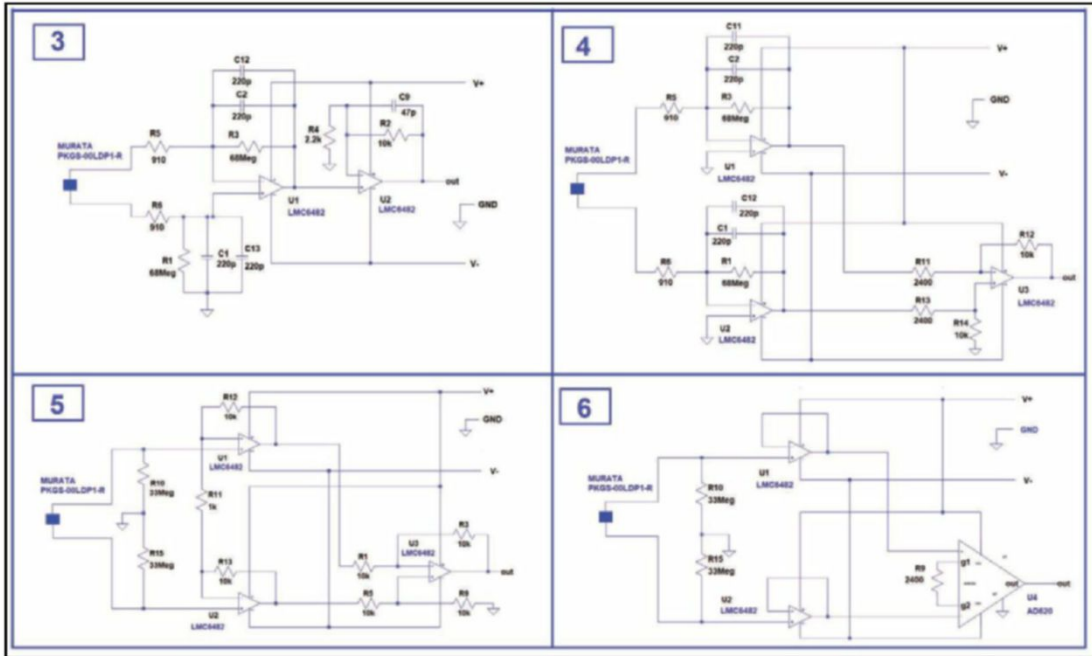


Figure 1: I tested four circuits and here are the schematics for each of them.

Photo 2 shows three of them. The first consists of two parallel sensors connected to the amplifier with a twisted pair to improve the rejection of the external electromagnetic interference.

The second arrangement is similar to the first one but with four parallel sensors to further improve the sensitivity. The third consists of two sensors connected in series with their common point connected through the shielding of the twisted pair cable to the ground of the amplifier circuit. The other two points are connected to the amplifier's positive and negative inputs.

As expected, the use of the shielded cable considerably improved the immunity to the external electromagnetic interference. I had even better results when I completely shielded the sensor with a metal can. I will give more detailed information about this in the next paragraphs.

The Sensor Connecting Cable

In every application, where the sensor is not next to its amplifier circuit, the cable is a major item effecting the system's noise performance. Especially for the piezoelectric acceleration sensor, the cable is much more critical and it is very important to select the proper cable to carry the high impedance signal.

"Tribo-electric" noise originates from capacity and charge changes due to dynamic bending, compression, and tension of the layers making up the cable. Common cables, when flexed or bent, generate an electrostatic charge output that is due to the layers making up the cable. This charge may have greater amplitude than the signal being generated by the accelerometer and the charge amplifier cannot separate whether the charge-generated signal is from the accelerometer or the

cable, so any disturbance of this kind should be eliminated by choosing and using the proper cable.

It is also equally important to make the cable as vibration-free as possible since the cable movements generate noise that interferes with the original signal. I use masking tape to firmly attach the cable because it allows easy removal without leaving residue or damaging to the loudspeaker cone. A good example of my technique is shown in **Photo 3**.

I have to admit that I spent more time looking for and testing the proper cable than I spent on the sensor itself. A lot of problems that I had during the first experiments with the sensors were due to the connecting cable and it took me some time

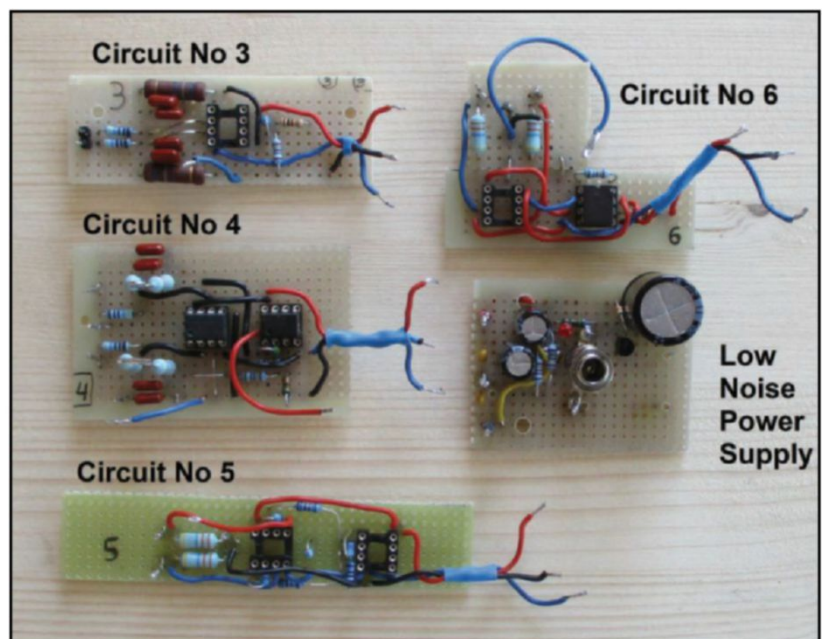


Photo 1: This is the construction of these circuits on prototype PCBs.

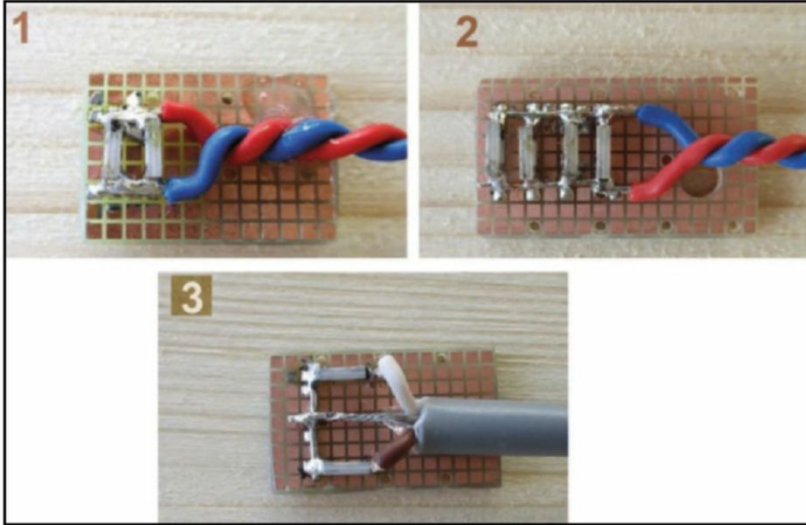


Photo 2: Here are three of different sensor arrangements that I tested while trying to increase the output level and possibly to find a layout that will reduce the mains interference.



Photo 3: Masking tape is used to firmly attach the cable.

to understand and figure out how to solve these problems. For example, in the measurement shown in **Figure 2**, the difference in response between the blue and the red curve is caused because a small part of the connecting cable was not supported well and it was free to move around.

When I noticed the cable used by the ACH-01 was produced by Mogami, I found the company's catalog and start searching for the proper cable. The problem was that the ultra-flexible and soft miniature cables that probably were suitable for the sensor could only be ordered in very large quantity, usually a 1000' reel.

After some research, I found a vendor from

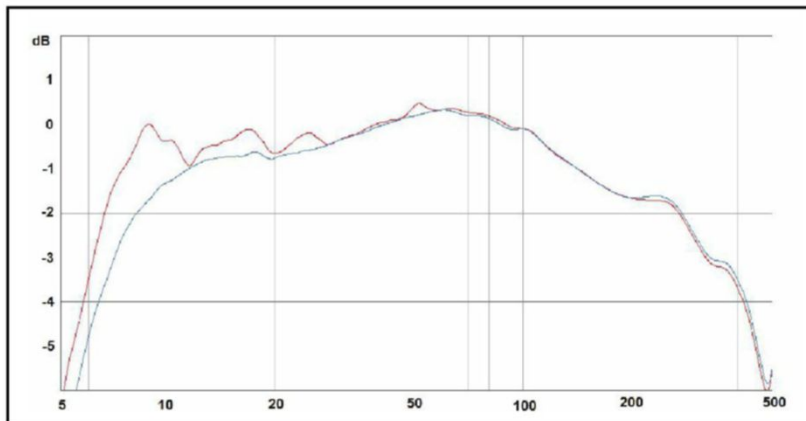


Figure 2: The difference in response between the blue and the red curve is caused because a small part of the connecting cable was not well supported and it was free to move around.

whom I could order a few types of Mogami cables in small quantities. I purchased and tested several of them and I ended up with the Mogami W2901 cable. This miniature, soft, and flexible cable that features mechanical strength is for use mainly in lavalier microphones. It has a outer diameter of only 2.16mm and a balanced configuration using two 0.054 mm² (#30 AWG) conductors and a double shield. I used a short length of about 60cm of this cable to connect the sensor to the amplifier.

The PZ-1 Sensor

As I mentioned, my initial tests were performed with the Murata PKGS-00LDP1-R shock sensors. I was just starting to design a small PCB for the sensor when Murata announced that it was going to discontinue the PKGS-00LDP1-R.

Fortunately, I did find that there was a possible replacement, the Murata PKGS-00GXP1-R (Mouser, #81-PKGS-00GXP1-R-R). The Murata PKGS-00GXP1-R is also a surface-mounted component with smaller dimensions (3.8 mm × 2mm × 1mm).

Its sensitivity is lower at 0.35 pC/g (±15%) and the capacitance is only 390pF (±30%). The resonance frequency is higher at 31kHz (±16%) but it is very strong in amplitude, almost +40dB and with a very high Q. This resonance will be compensated by the amplifier's electronic circuit. **Photo 4** shows a comparison between the two sensors.

I designed a small double-sided PCB for easy mounting of the Murata sensors and the cable. The PCB has a ground plane on its bottom side and the Murata sensors are placed on its top side. Small pads are included for the connection of the connecting cable as shown in the right side of **Photo 5**. The two sensors are connected in parallel. The ground plane of the sensor PCB is connected through the shielding of the cable to the ground of the amplifier. The sensor has a polarity marking indication on its body and each sensor should be placed on the PCB with the same polarity, otherwise cancellation of their outputs will occur because they are connected in parallel.

Photo 5 shows how the assembly of the sensor was done. On the left side (a), the cable was prepared for soldering on the PCB of the sensor. In the middle (b) are the pins and the connector that was used for the connection of the cable to the amplifier. The right side (c) shows the small PCB of the sensor with the Murata sensors soldered on its position. The left side of **Photo 6** shows the completed sensor, which I named PZ-1.

The PZ-1-sh Sensor

The PZ-1 sensor with the Mogami cable gave very

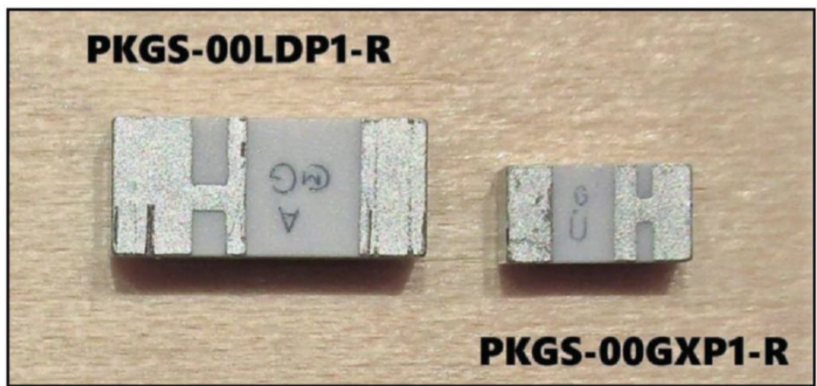


Photo 4: I compared the Murata PKGS-00LDP1-R shock sensors, which has discontinued and its potential replacement, the Murata PKGS-00GXP1-R.

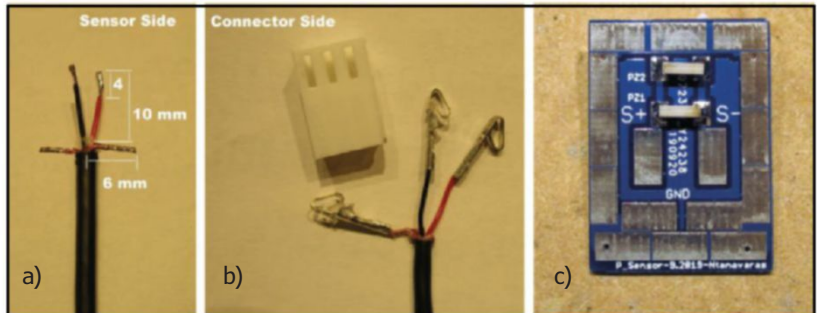


Photo 5: To assemble the sensor, I prepared the cable for soldering on the PCB of the sensor (a); in the middle are the pins and the connector that was used for the connection of the cable to the amplifier (b); and the right side shows the small PCB of the sensor with the Murata sensors soldered on its position (c).

Loudspeaker Design Cookbook
7th edition
BY Vance Dickason
NEW SEVENTH EDITION

Everything you Need to Become a Better Speaker Designer

Build Your DREAM SPEAKER!
Four: • Home • Car • Home Theater

PLUS – PLANS FOR

- A Complete Home-Theater System
- A Studio Monitor

The “Must Have” reference for loudspeaker engineering professionals.

Back and better than ever, this 7th edition provides everything you need to become a better speaker designer. If you still have a 3rd, 4th, 5th or even the 6th edition of the Loudspeaker Design Cookbook, you are missing out on a tremendous amount of new and important information! **Now including: Klippel analysis of drivers, a chapter on loudspeaker voicing, advice on testing and crossover changes, and so much more!**

A \$99 value!
Yours today for just \$39.95.

www.cc-webshop.com

Photo 6: The PCB of the PZ-1 sensor was designed so that the metal can could be soldered directly to its ground plane. Here, the sensor is shown with the metal can before it was soldered to the PCB.

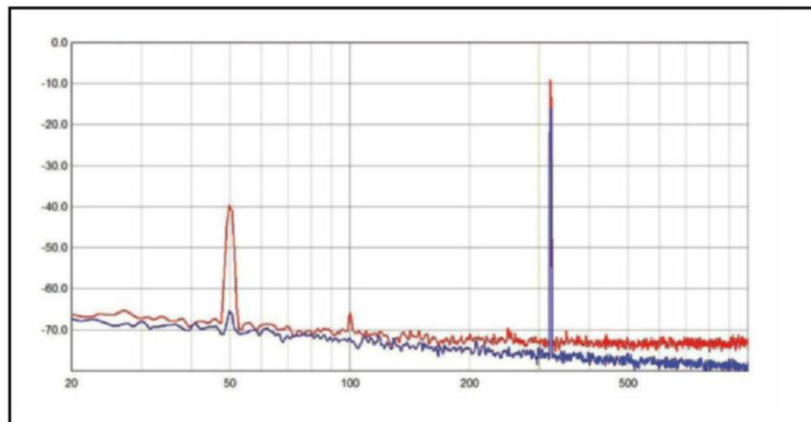
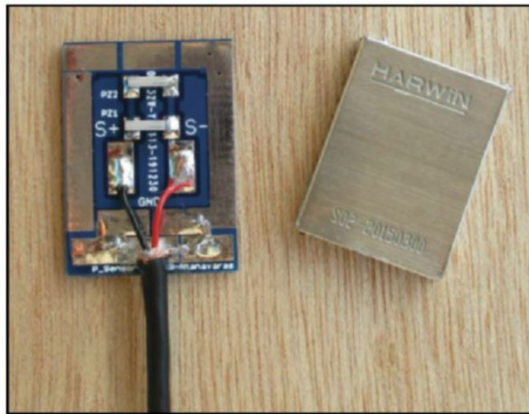


Figure 3: This graph shows a comparison of the frequency spectrum at the output of the piezoelectric amplifier between the PZ-1 and the PZ-1-sh sensors.

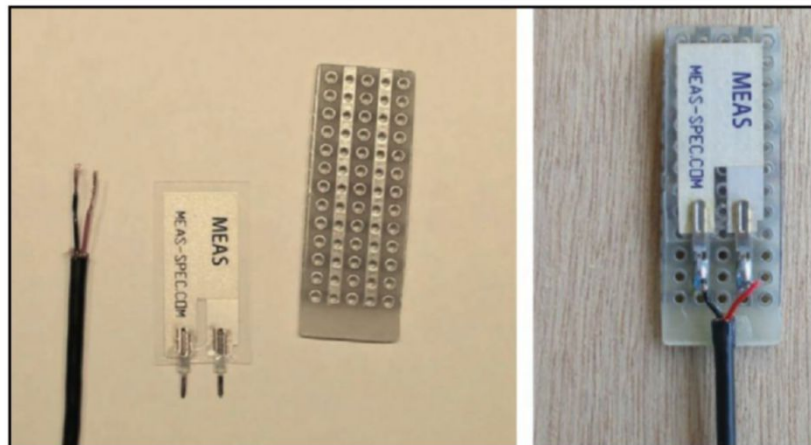


Photo 7: A small PCB was cut and permanently glued to the sensor using Loctite 401 instant adhesive (PZ-2-Parallax sensor).

About the Author

George Ntanavaras graduated from the National Technical University, Athens, Greece, in 1986 with a degree in Electronic Engineering. He currently works as a Technical Consultant for Greek electronics companies. He is interested in the design of preamplifiers, active crossovers, power amplifiers, and most loudspeakers. He also enjoys listening to classical music.



good results concerning the suppression of the mains interference. I found out that the results were further improved when I used a small electromagnetic compatibility (EMC) shield can to completely shield the sensor. This is a EMC shield nickel can with dimensions of 20mm × 15mm × 3mm and thickness at 0.2mm (Harwin S02-20150300).

I designed the PCB of the PZ-1 sensor so that the metal can could be soldered directly to its ground plane and I named this version of the sensor PZ-1-sh. Photo 6 shows the sensor with the metal can before it was soldered to the PCB.

The metal can further eliminate the mains interference and also reduced the total output noise of the amplifier. **Figure 3** shows a comparison of the frequency spectrum at the output of the piezoelectric amplifier between the PZ-1 and the PZ-1-sh sensors. Both of them were attached to the Peerless cone, which reproduced a 320Hz sine signal. With the shielded sensor, the 50Hz mains interference is 25dB lower in level while the 100Hz is totally eliminated. The total noise floor is reduced by 2dB to 3dB.

The PZ-2-Parallax Sensor

After I had very good results with the PZ-1 and PZ-1-sh sensors, I decided to look for some other ready-made sensors that could be used. The Parallax Vibration tab sensor #605-00004 (Mouser 619-605-00004) consists of a flexible piezoelectric film laminated to a polymer substrate. When the sensor is bent or displaced from its neutral axis, the strain within the piezoelectric film generates voltage. According to its datasheet, the device has a high sensitivity of 50 mV/g and can generate very large voltages up to 70V if bent to 90°.

I cut a small PCB with dimensions of 38mm × 14mm as shown on the left side of **Photo 7**, where I permanently glued the sensor using Loctite 401 instant adhesive. In this way, the sensor cannot bend and produce high voltages.

I used a Mogami W2901 cable to connect the PCB to the amplifier. The two pins of the sensor were connected to the positive and the negative input of the amplifier. The shield of the cable was connected only to the ground of the amplifier. I also glued the cable to the sensor PCB using Loctite 401. I named this sensor assembly PZ-2-Parallax.

The amplifier that I will present in the third part of the article series was specially designed for the PZ-1 and PZ-2-sh sensors. I conducted all the tests for this sensor using this amplifier without any problems, but I used low vibration levels. Probably at higher levels, some protection will be needed and the following modifications will be sufficient, although I have not applied them.

The datasheet of the Parallax sensor recommends that a series 220 Ω resistor with a parallel clamping Zener diode of 5.1V should be connected at the output of sensor to protect the next circuit. I think the amplifier will be also effectively protected if its input resistors R1 and R20 are increased to 1k Ω and two parallel connected ultra low leakage diodes with reverse polarities are placed between the (+) and (-) pins of the IC1A. Also the gain of IC1B should be reduced to 0dB by omitting resistor R30.

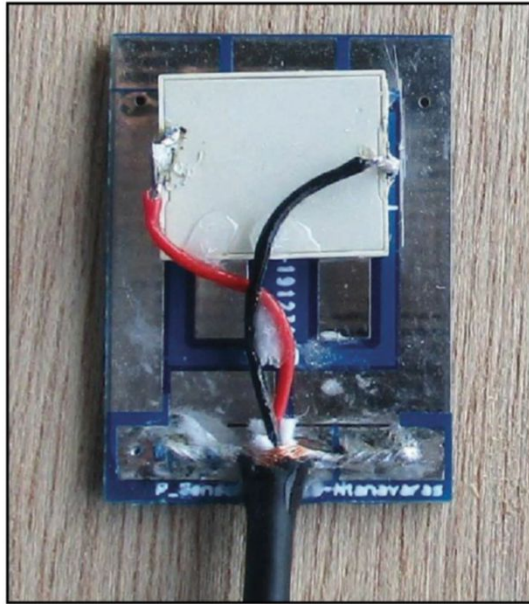


Photo 8: A Mogami W2901 cable was used to connect the PCB to the amplifier (PZ-3-PUI sensor).

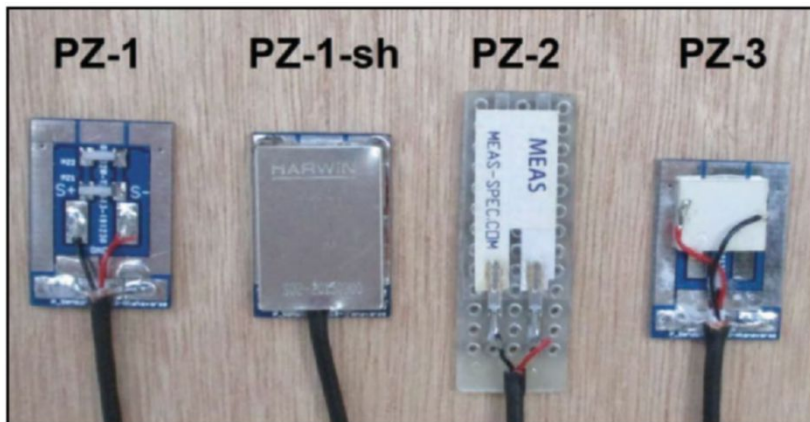


Photo 9: Here are all four sensors that were described in this article.

Sources

Mogami Cables | www.mogamicable.com/category/bulk

Murata Manufacturing Co., Ltd. | www.murata.com/en-sg/products/sensor/shock

Parallax, Inc. | www.parallax.com/product/605-00004

PUI Audio, Inc. | www.puiaudio.com/products/smt-1141-t-5-r

The PZ-3-PUI Sensor

A piezoelectric speaker is a loudspeaker that uses the piezoelectric effect for generating sound. The motion that produces the sound is created by applying a voltage to a piezoelectric material. Typically they operate in the range of 1kHz to 5kHz, and they are used to generate sounds in electronic devices or as tweeters in computer speakers and portable radios.

PUI Audio SMT-1141-T-3-R (Mouser, #665-SMT-1141-T-3-R) is a surface-mounted piezoelectric loudspeaker with very small dimensions (11mm \times 9mm \times 1.7mm). It has a resonance frequency at 4.1kHz and a very high capacitance of 12000pF (\pm 30%). It weighs only 0.3 grams.

I permanently glued it with Loctite 401 instant adhesive on the PCB that I designed for the PZ-1 sensor and I used a Mogami W2901 cable to connect the PCB to the amplifier as shown in **Photo 8**. The cable was also glued to the PCB.

The measurements proved that this type of sensor was a lot more sensitive than the others, having an output almost 35dB higher than the ACH accelerometer. Taking into consideration that the capacitance of this sensor is more than 30 times bigger, this is something that should have been expected. I have to test it with very low vibration levels to avoid overloading the amplifier.

Unfortunately, just before I finished writing the article, I found out that this transducer was obsolete. The SMT-1141-T-5-R (Mouser #665-SMT-1141-T-5-R) has exactly the same characteristics and although I have not tested it, I think it will probably give similar results. The modifications for the protection of the amplifier as described in the paragraph about the PZ-2-Parallax sensor are also valid here. Additionally, the gain of IC1A should be reduced.

Other Transducers

All four sensors that were described in this article are shown in **Photo 9** for comparison. Of course, there are a lot of other piezoelectric sensors on the market that I have not tested it and they would probably also give good measurements results.

Some other sensors that I ordered for testing that gave good measurements results are shown in **Photo 10** (from left to right): Measurement Specialties SDT-028K (Mouser, #824-1-1000288-0), Measurement Specialties FDT1-028K (Mouser, #824-1-1002785-1), and Measurement Specialties LDT1-028K sensors (Mouser, #824-1-1002910-0).

The SDT1-028K is an interesting sensor. It is fully shielded for use in applications in high electromagnetic interference (EMI) environments. It consists of a rectangular element of piezo film

together with a molded plastic housing and 18" of coaxial cable. The film element, screen printed with silver ink, is folded over on itself, providing self-shielding of the sensor area. The dimensions of the sensor are: Length=28.6mm, Width=11.2mm, and Height=0.13mm.

The FDT1 Sensor is a rectangle element of Piezo film with with 28µm thickness and silver ink screen printed electrodes. Rather than making the lead attachment near the sensor, the piezo polymer tail extends from the active sensor area as flex circuit material. This gives a very flat, flexible lead with a connector at the end.

The LDT1 sensor has a piezo film element laminated to a sheet of polyester (Mylar). The dual wire lead attached to the sensor transfers the signal.

All these sensors are suitable for vibration measurements but depending on the surface, special attention will be needed to properly mount them.

Next Month

In the final part of this article series, I will describe the design and the construction of the piezoelectric amplifier and the measurements that will enable us to evaluate the whole system. ☒

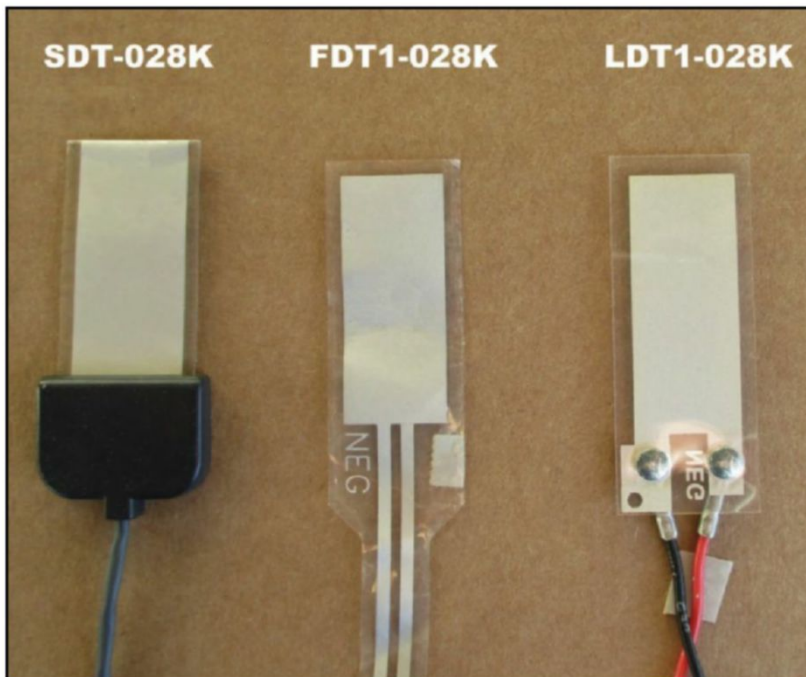


Photo 10: These are some other sensors that were used for testing and provided good measurements (from left to right): Measurement Specialties SDT-028K, Measurement Specialties FDT1-028K, and Measurement Specialties LDT1-028K sensors.

**GETTING THE MOST OUT OF
VACUUM
TUBES**

By Robert B. Tomer

Vacuum Tubes—The Important 4/5ths of Tube Circuits
Over 80% of all tube equipment defects result, directly or indirectly, from tube failures. Why do tubes fail? What can be done to prevent them from failing before their time? How can you determine whether a tube is good or bad, or how well and how long it will work in a given circuit? Should tubes be replaced periodically, whether they've failed or not . . . or should they be tested every so often, and replaced if indications show them to be below par? This book supplies the answers to these profound questions . . . plus many, many more.

Like Watching a Play From Backstage
Author "Bud" Tomer, an international authority on tubes, is well-known for his candid "Tech Tip" bulletins and his slide-film presentations to service, military and engineering groups. Within this book you'll find a virtual encyclopedia on vacuum tubes—yet the author has not delved into mathematical details that would be of interest to only a few tube engineers. Everything is focused toward the interest of those who use tubes—either for replacement purposes or in original equipment designs.

In his refreshing, down-to-earth style, Mr. Tomer sheds light on the "Why so many tube types?" "What About Tube Testers?", etc.

Other Interesting and Informative

- 10 reasons why tubes fail
- Predicting tube performance
- Selected and preferred tube types
- Lengthening tube life

Anyone who has anything at all to do with tube equipment design, or proper use—should read this book. It is a must for anyone who designs, maintains, repairs, produces and manufacturing processes—or even uses vacuum tubes in their computers and radar gear.

You'll also learn about

- Catastrophic failures—what they are, when and why they occur
- Degenerative failures—what happens to tube electrodes
- Subjective failures—why a seemingly normal tube may be defective
- Characteristic variables—differences that make one tube better than another
- Special-purpose tubes—considerations for filament, diode, and thyratron types.

**Order your copy
at
cc-webshop.com**

DO IT YOUR WAY

Cables/Panels/Boxes

WITH REDCO AUDIO'S

"Build Your Own" web pages

Full control for design, editing and more.

AND WE'LL BUILD IT JUST THE WAY YOU WANT!

REDCO AUDIO

www.redco.com 203-502-7600

Measuring Vibration with Piezoelectric Sensors (Part 3)

The Piezoelectric Amplifier

By
George Ntanavaras



In the third and final part of this article series, George Ntanavaras describes the design and construction of the piezoelectric amplifier and presents the measurements he took to evaluate the system.

I designed a piezoelectric amplifier especially for the PZ-1 sensor, but other piezoelectric sensors could be connected although some modifications might be needed. The electronic diagram of the piezoelectric amplifier is shown in **Figure 1**.

A detailed description of the operation of the circuit follows:

- At the input of the circuit, there is a 3-pin connector for the sensor—the first is the positive input (IN-1); the middle is the ground pin (IN-2); and the third is the negative pin (IN-3).
- The differential charge amplifier is built around op-amp IC1A. Resistors R1 and R20 offer some protection against possible over-voltages at the input of the amplifier. Capacitors C1-C4 and C19-C22 adjust the gain of the amplifier while resistors R2-R5 and R21-R24 are used to properly bias the op-amp. I used four parallel connected capacitors and four series connected resistors to achieve better matching for the total values of the positive and negative side

since this affects the common mode voltage rejection of the circuit.

- IC1 has to be an ultra-low input current operational amplifier and I used in this position the CMOS dual op-amp LMC6482. It has a input current of 20fA, a rail-to-rail output swing, a high input impedance, a large common-mode range and a high CMRR. The last two are very important for the differential circuits. According to its datasheet, the circuits designed with the LMC6482 can reject a larger range of common-mode signals than others making them an excellent choice for operation in noisy environments.
- IC1B provides an additional gain of 16dB to the signal. C31 with R26 form a low-pass filter at around 40kHz to reduce the bandwidth and the high frequency noise.
- Switch S1 selects between 3Hz, 16Hz, or 160Hz for the cut-off frequency of the first-order high-pass filter that is formed with capacitors C6, C10, C11, and R15. The IC2A buffers the high-pass filter and through switch S2 provides

different gains between 0dB, 10dB, and 20dB by selecting resistors R32, R33, R34 as feedback for the IC2A.

- The components around IC2B and IC3A form a two-stage sixth-order low-pass filter with the -3dB point at 12kHz. This gives an attenuation of about 37dB at 31kHz and suppresses the very high Q resonance of the PKGS-00GXP1-R sensor to achieve a more flat response.

For a better understanding of the next circuits, let's refresh our memory with the basics of the simple harmonic oscillation theory. Suppose an object oscillates periodically with a frequency f and the instantaneous value of the excursion (=displacement) is given as the function of time by $x(t)$. We can calculate the velocity $v(t)$ of the object as the first derivative of the excursion and the acceleration $a(t)$ as the first derivative of the velocity or the second derivative of the excursion.

Now let's think the opposite, supposing that the acceleration $a(t)$ is known. The velocity can be calculated by integrating the acceleration signal over time while the excursion by integrating the velocity over time. This is our case—the sensor gives the acceleration and we need an integrator to calculate the velocity. This can be realized very easily with an electronic integration circuit based on an op-amp, a capacitor, and a resistor. It is similar to an active low-pass filter with a very low cut-off frequency.

The amplifier includes two such integrator circuits in series—one for the calculation of the velocity and another for the excursion.

The op-amp IC3B with R6 and C5 form the first integrator that gives at its output the velocity of the input signal. Resistor R7 is in parallel with the integration capacitor C5 limiting the gain of the circuit at the very low frequencies to a finite value.

The op-amp IC4A with R31 and C23 form the second integrator that gives at its output the excursion (=displacement) of the input signal.

Switch S3 selects the type of the signal that will be connected to the output of the amplifier. Resistors R27, R29, R36 form dividers with R28 properly adjusting the level of the output signal. IC4B is a unity gain buffer that drives the selected signal to the output connector.

The conversions factors between the level of the output voltage and the absolute values of the measured quantities were defined as follows:

- acceleration 1 mVrms corresponds to 1m/sec²
- velocity 1 mVrms corresponds to 0.01m/sec
- excursion 1 mVrms corresponds to 0.01mm

These factors are valid only for the the PZ-1 sensor supposing that the Murata sensor has its nominal sensitivity. The large tolerances of the Murata sensor used in PZ-1 and PZ-1-sh sensors, ($\pm 15\%$ for its charge sensitivity and $\pm 30\%$ for its capacitance), cannot allow a very accurate output, so the above factors should be taken only as indicative. The amplifier's gain was adjusted so that when the PZ-1 sensor is connected at its input, the voltage at the acceleration output will be similar to the voltage

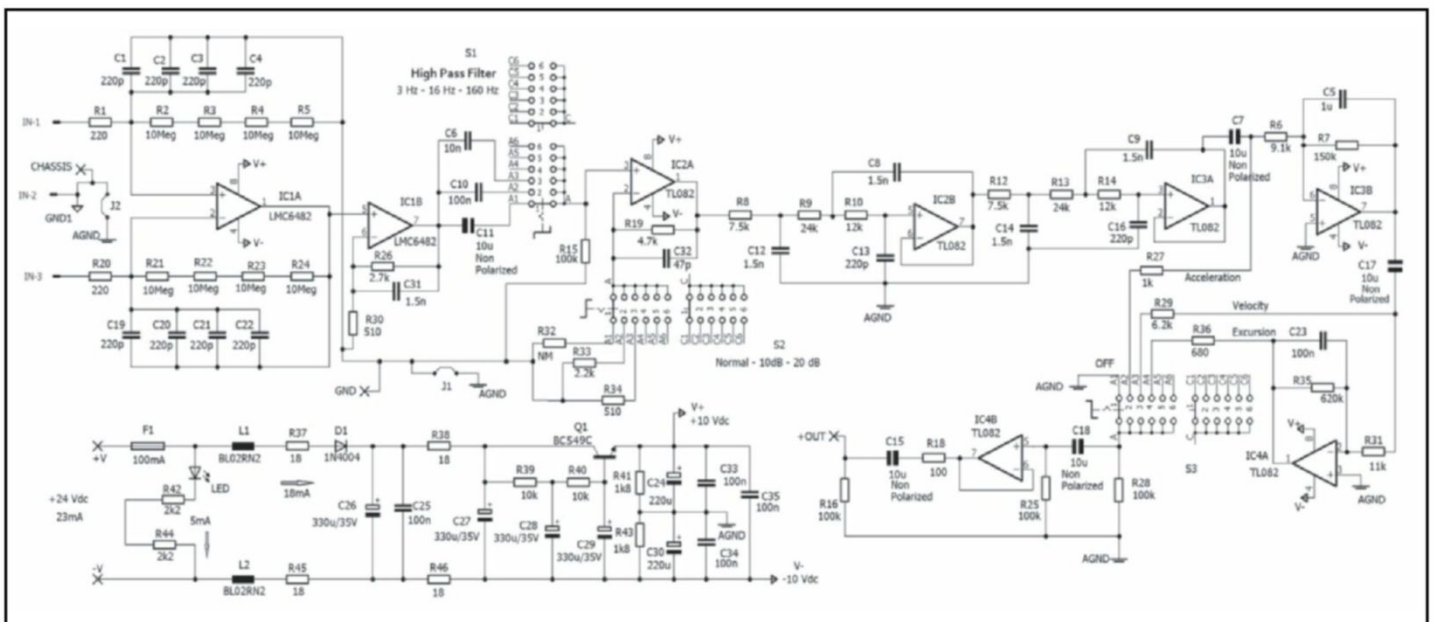


Figure 1: This is the electronic diagram of the piezoelectric amplifier.

About the Author

George Ntanavaras graduated from the National Technical University, Athens, Greece, in 1986 with a degree in Electronic Engineering. He currently works as a Technical Consultant for Greek electronics companies. He is interested in the design of preamplifiers, active crossovers, power amplifiers, and most loudspeakers. He also enjoys listening to classical music.



that will be produced by the ACH accelerometer when connected to its amplifier.

The gains of the integrators for the velocity and the excursion were adjusted to meet the previously mentioned conversions factors.

The amplifier needs 24 VDC for its operation and has a low consumption at about 23mA out of which the 5mA are used for the power LED indication. I used a small Desktop AC adapter from XP Power, type VET18US240C2-JA. It is a 18W switching power supply with 24 VDC/750mA output but any other power supply with low ripple will be suitable.

Fuse F1 is used for protection of possible excessive currents in case of a fault and when the external power supply has no short circuit protection. L1 and L2 are ferrite beads with lead wires to attenuate the very high frequencies for suppression of EMI noise. Diode D1 assures that the input voltage will be connected to the amplifier with the correct polarity. Resistors R37, R38, R45, R46 with capacitors C25-C27 form low-pass filters to additionally suppress the high-frequency noise of the power supply. Transistor Q1 forms a capacitance multiplier, which provides at its output a very low noise DC voltage of about ± 10 VDC for the supply of the circuit.

Resistors R41 and R43 are equal and their common point is the virtual ground of the circuit. Capacitors C24, C30, C33, C34 decouple the supply voltages improving the stability of the op-amps.

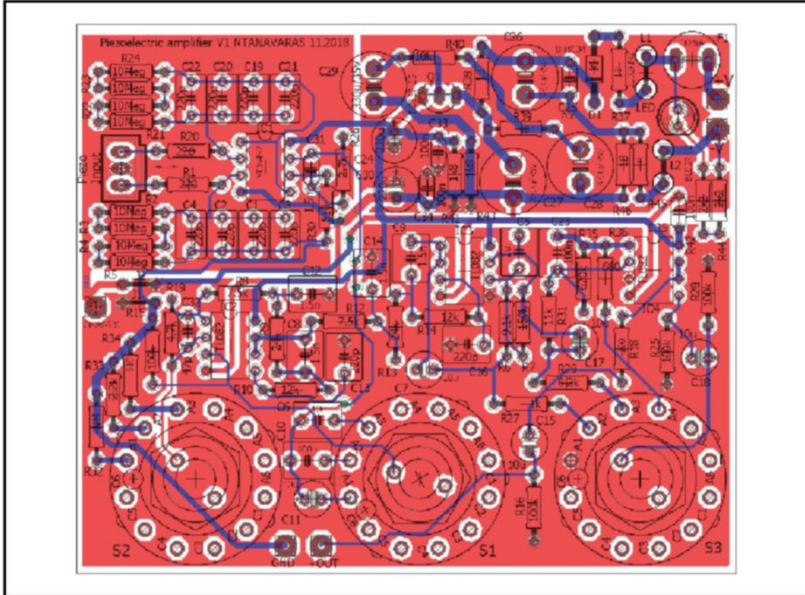


Figure 2: The dimensions of the PCB are 84mm x 101mm, and this board shows the placement of the components.

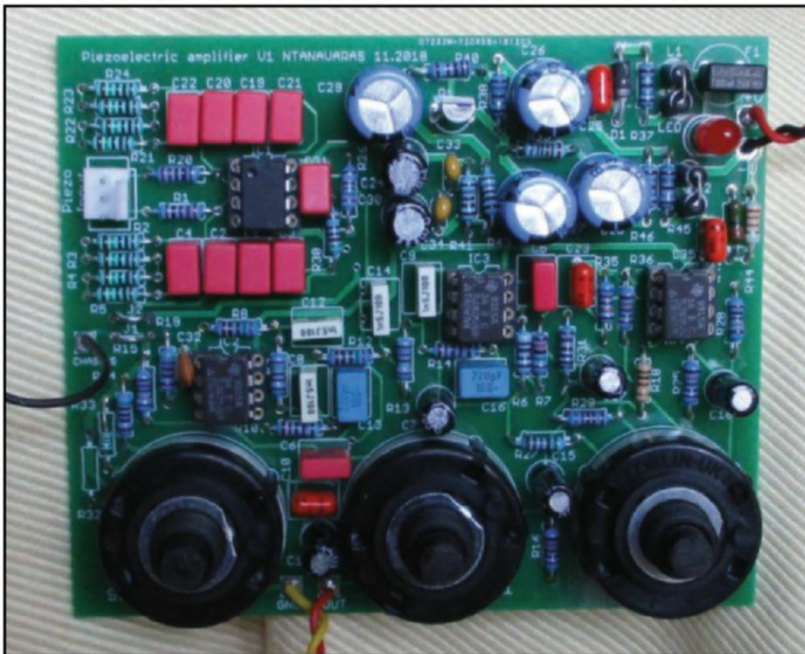


Photo 1: The assembled PCB shows the three rotary switches S1, S2, and S3 soldered directly on the PCB to facilitate the construction of the amplifier.



Photo 2: For the completed amplifier. I used the same metal box from Hammond and the aluminum frontplate that I had designed for the ACH-01 amplifier.

The Construction of the Amplifier

I designed the PCB for the amplifier using the Demo version of the Eagle Layout editor. This demo version of the program can be downloaded free of charge from the Cadsoft website (www.cadsoftusa.com). The demo version is fully operational except a limitation on the maximum dimensions of the PCB, which was not a problem for this project.

I ordered a high-quality PCB manufactured from FR4 composite material with a 1.6mm thickness and 35µm copper solder on both sides and silkscreen on the top side. The dimensions of the PCB are 84mm × 101mm and the placement of the components is shown in **Figure 2**. All the components are placed on the top side of the PCB.

Photo 1 shows the assembled PCB. The three rotary switches S1, S2, and S3 are soldered directly on the PCB to facilitate the construction of the amplifier.

I used good quality IC sockets for the op-amps on my prototype, but this is not necessary unless you are planning to test different types of op-amps. The three switches are fastened directly on the front panel and support the whole PCB. The output

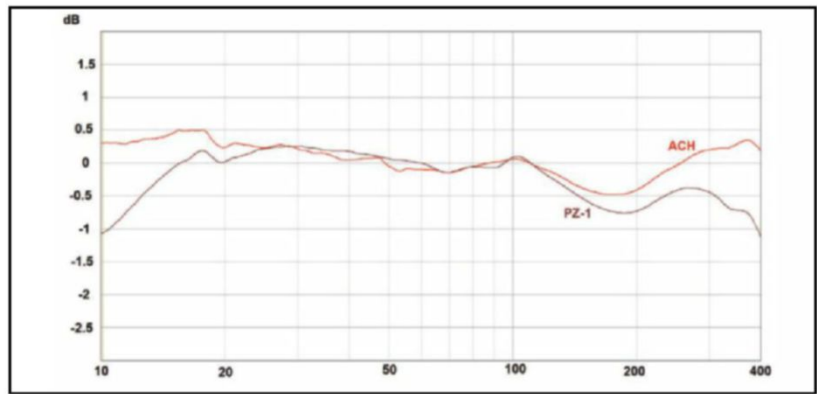


Figure 3: The graph shows a comparison between the acceleration response of the Peerless cone measured by the ACH and the PZ-1.

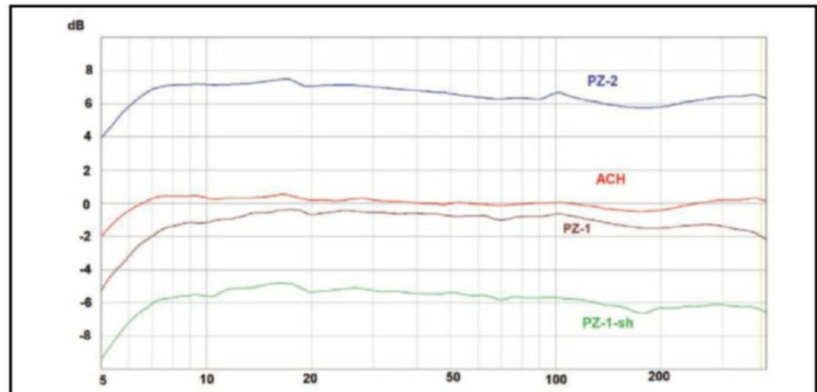


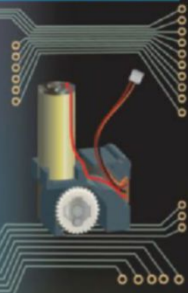
Figure 4: This graph details the acceleration of the Peerless cone as measured with the PZ-2, PZ-1, PZ-1-sh, and ACH without normalization.

ALL ELECTRONICS

CORPORATION

Thousands of Electronic Parts Available Today!

LEDS · CONNECTORS · RELAYS
SOLENOIDS · FANS · ENCLOSURES
MOTORS · WHEELS · MAGNETS
PC BOARDS · POWER SUPPLIES
SWITCHES · LIGHTS · BATTERIES
and many more items...



We have what you need for your next project.



www.allelectronics.com

Discount Prices · Fast Shipping

A²B Audio Modules

32 channels of digital audio over twisted pair

Accelerate Design Time:

- Development tools
- OEM modules
- I/O modules



CLOCKWORKS

Signal Processing

www.clk.works info@clk.works

+1 978 258 5402

A²B is a trademark of Analog Devices Inc.

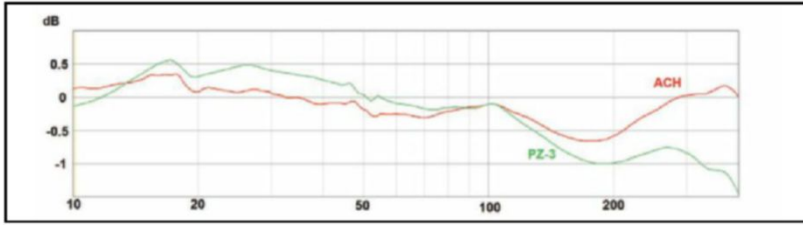


Figure 5: In this graph we compare the acceleration response of the PZ-3 and ACH sensors after they were normalized for equal level at around 100Hz.

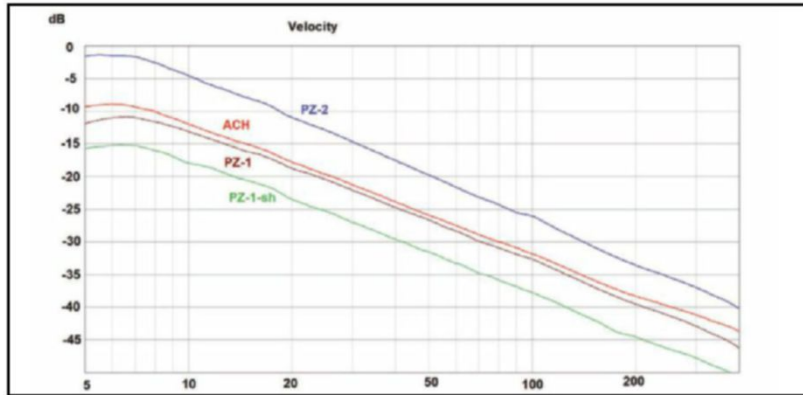


Figure 6: This graph details the velocity of the Peerless cone as measured with the four sensors without normalization.

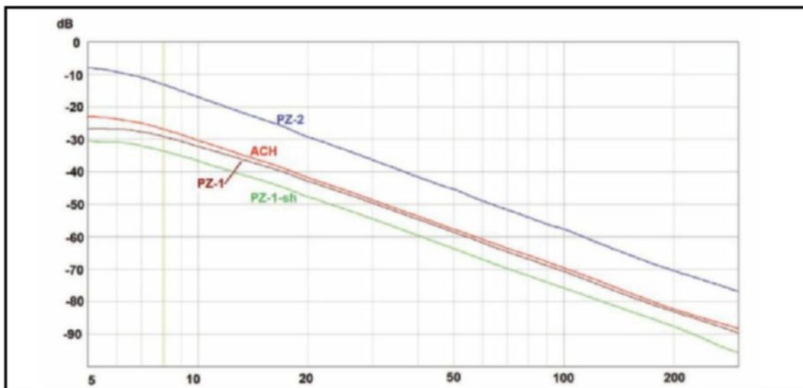


Figure 7: Here we see the excursion of the Peerless cone as measured with the four sensors without normalization.

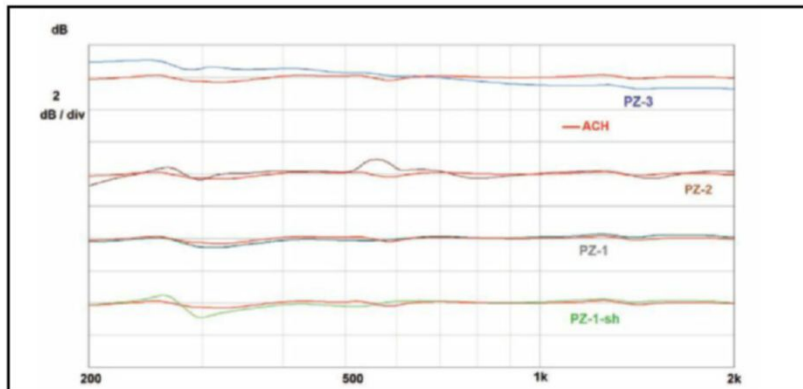


Figure 8: In this graph we see the acceleration of the Visaton exciter as measured with the four sensors.

connector and the supply connector are placed on the front panel.

The Parts List details the components required to build the amplifier. **Photo 2** shows the completed amplifier. I used the same metal box from Hammond and the aluminum frontplate that I had designed for the ACH-01 amplifier. This is an engraved front panel, which replaces the original top cover of the Hammond box. I placed two adhesive labels to cover the engraved text for the input of the ACH and the power supply as shown in Photo 2, since they are different for this amplifier. The ground point of the PCB of the amplifier is connected with a short wire to the metal box chassis to ensure better shielding.

The Sensor Placement

Proper placement of the piezoelectric sensor on the vibrating surface is very critical—a sensor installed incorrectly can give very wrong results.

The ACH manufacturer recommends to use a quick setting viscous methyl cyanoacrylate adhesive or any epoxy adhesive. This should be applied sparingly to the clean surface and should be allowed to set.

This is an excellent method for permanent placement but not for temporary use. Although the manufacturer recommends to avoid soft adhesives, such as double-sided tape because they can adversely affect the ACH performance, this is the only method I have found to use for temporary measurements. My preference is a standard thin double-sided tape from Tesa, which is strong enough to hold the sensor in good contact with the surface but allows it to be carefully removed. This is something that requires some experience but it works.

As I already have mentioned, another very important point is that the part of the cable that is close to the sensor should be adhered firmly to the surface and not allowed to move at all.

Measurements with Sensors

For the final evaluation of the system, I will present some of the measurements that I took with the piezoelectric sensors attached to the Peerless cone for the frequency range between 5Hz and 400Hz and on the Visaton Bass Exciter for the frequency range between 200Hz and 2kHz.

Figure 3 shows a comparison between the acceleration response of the Peerless cone measured by the ACH and the PZ-1. The two curves were normalized for equal level at 70Hz for easy comparison. They have very similar response, within 0.5dB, between 17Hz and 220Hz. Probably, they have very similar response above 220Hz, but

the break-up mode of the subwoofer's cone (not shown) starts to influence each measurement in a different way since it occurs at very different frequencies, 720Hz for the ACH and 910Hz for the PZ-1.

Figure 4 shows the acceleration of the Peerless cone as measured with the PZ-2, PZ-1, PZ-1-sh and ACH without normalization. The PZ-2 is 6dB to 7dB more sensitive than the ACH. The responses of the ACH and PZ-1 are very close, with the PZ-1 less sensitive for about 1dB. Considering the large tolerance of the Murata sensor, this is a very nice result. The shielded sensor PZ-1-sh is 5dB to 6dB lower in sensitivity than the ACH. Both the PZ-1 and PZ-1-sh have less than 1dB difference from the response of the ACH, when their responses are normalized.

The PZ-3 sensor is much more sensitive than the other sensors, almost 35dB higher. **Figure 5** compares the acceleration response of the PZ-3 and ACH sensors after they were normalized for equal level at around 100Hz. They are very similar.

Figure 6 shows the velocity and **Figure 7** shows the excursion of the Peerless cone as measured with the four sensors without normalization. The responses are very close.

I also measured the distortion of the Peerless cone's acceleration and the results were very similar for all four sensors.

Figure 8 shows the acceleration of the Visaton exciter as measured with the four sensors. Here I placed the response of the ACH normalized at the same level to the responses of each sensor for easy comparison. Again the response of PZ-1 and PZ-1-sh are almost identical to the response of the ACH. The small deviation in the response of the PZ-1-sh around 280Hz is probably some minor resonance due to the placement.

Figure 9 shows the velocity, and **Figure 10** shows the excursion of the Visaton exciter as measured with the sensors. The responses were again normalized to have the same level. It should be noted that the measurement of the excursion is very difficult at the higher frequencies because the signal levels are much lower in level.

Another example that will interest a lot of loudspeaker builders is shown in **Figure 11**—a panel vibration measurement of a loudspeaker cabinet. It was measured by attaching each accelerometer to the same point at the front panel of a well-braced cabinet. I used the ARTA software producing a pink noise signal and a power amplifier to drive the loudspeaker at a high sound level. The piezoelectric amplifier gain was set to 20dB gain because the signals were very low in level. The red curve

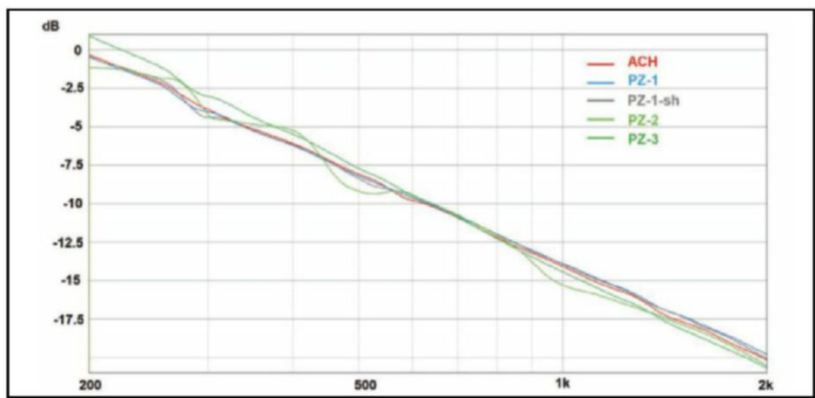


Figure 9: This graph shows the velocity of the Visaton exciter as measured with the sensors.

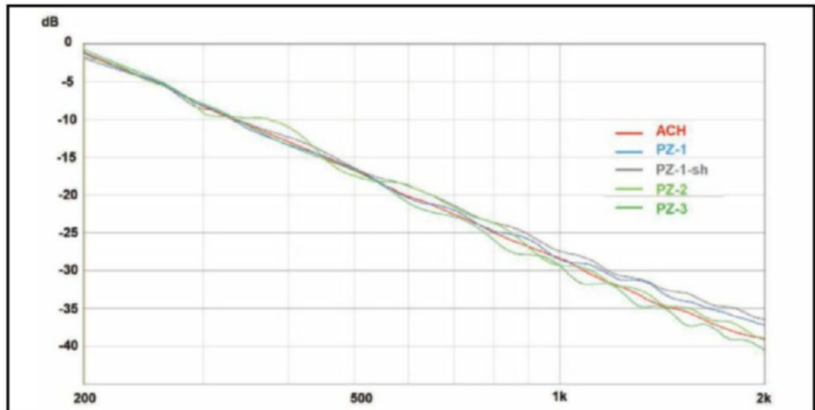


Figure 10: In this graph, we see the excursion of the Visaton exciter as measured with the sensors.

We are a world leading manufacturer of high performance transformers for audio applications. Let us help you improve your sound.

"IF YOU CAN HEAR IT, IT'S NOT OURS"

LUNDAHL
— TRANSFORMERS —

LUNDAHL
— TRANSFORMERS —

www.lundahltransformers.com
office@lundahltransformers.com

represents the measurement with the ACH, the blue curve represents the measurement with the PZ1, and the green curve represents the measurement with the PZ-1-sh. The curves shown were offset by several decibels for clarity and they were very

similar, clearly showing the main panel resonance at around 300Hz. An interesting point is that in the response of the PZ-1-sh sensor, the 50Hz mains interference is almost eliminated.

Conclusion

This was a very long journey on which I have learned a lot of interesting things. I believe that the outcome resulted in a very simple-to-build system that is able to generate useful measurements, concerning the acceleration, the velocity, and the excursion of a vibrating surface of a loudspeaker cone, a loudspeaker panel, or a turntable. If you are looking for an easy way to begin exploring vibration measurements, building this system will be a good start.

Author's Note: I have a few PCBs available for the construction of the piezoelectric amplifier and the PZ-1 sensor. Anyone who is interested can please send me an email at: gntanavaras@gmail.com

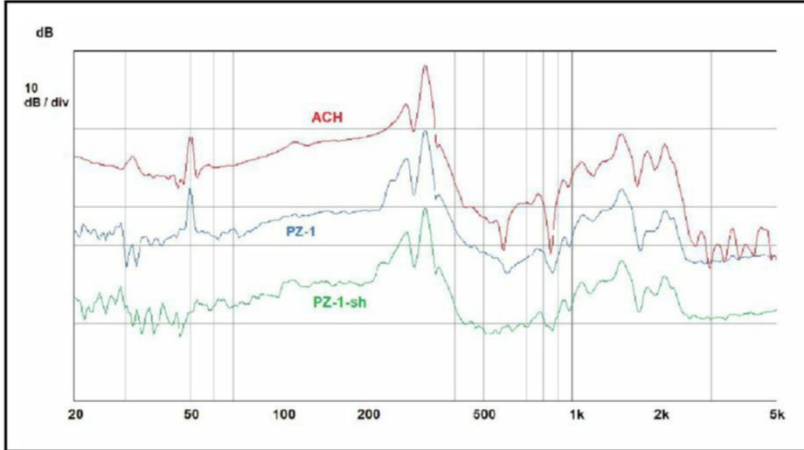


Figure 11: I measured the panel vibration of a loudspeaker cabinet by attaching each accelerometer to the same point at the front panel of a well-braced cabinet

Parts List for the Piezoelectric Amplifier

Part	Value	Notes	Part	Value	Notes
C1, C2, C3, C4, C13, C16,			R8, R12	7.5kΩ	Metal film, 0.25W, 1%
C19, C20, C21, C22	220pF, 100V, 2.5%	Polypropylene	R9, R13	24kΩ	Metal film, 0.25W, 1%
C5	1u	Plastic film	R10, R14	12kΩ	Metal film, 0.25W, 1%
C6	10n	Plastic film	R15, R16, R25, R28	100kΩ	Metal film, 0.25W, 1%
C7, C11, C15, C17, C18	10u / 16V	Non Polar Electrolytic	R18	100Ω	Metal film, 0.25W, 1%
C8, C9, C12, C14, C31	1.5n	Plastic film	R19	4.7kΩ	Metal film, 0.25W, 1%
C10, C23	100n	Plastic film	R26	2.7kΩ	Metal film, 0.25W, 1%
C24, C30	220u / 16V	Electrolytic	R27	1kΩ	Metal film, 0.25W, 1%
C25, C33, C34, C35	100nF	Ceramic	R29	6.2kΩ	Metal film, 0.25W, 1%
C26, C27, C28, C29	330u / 35V	Electrolytic	R30, R34	510Ω	Metal film, 0.25W, 1%
C32	47p	Ceramic	R31	11kΩ	Metal film, 0.25W, 1%
D1	1N4004	Diode	R32	Not placed	
F1	Fuse 100mA	Fuse for PCB	R33, R42, R44	2.2kΩ	Metal film, 0.25W, 1%
IC1	LMC6482	Op-amp	R35	620kΩ	Metal film, 0.25W, 1%
IC2, IC3, IC4	TL082	Op-amp	R36	680Ω	Metal film, 0.25W, 1%
IN	Header, vertical	3-pin, 1 row	R37, R38, R45, R46	18Ω	Metal film, 0.25W, 1%
L1, L2	BL02RN2R1M2B	Ferrite Beads	R39, R40	10kΩ	Metal film, 0.25W, 1%
LED	red	5mm	R41, R43	1.8kΩ	Metal film, 0.25W, 1%
Q1	BC549C	Transistor	S1, S2, S3	Switch, 2-Pole, 6-Position CK1060	
R1, R20	220Ω	Metal film, 0.25W, 1%	Metal box	Hammond 1590XXBK	
R2, R3, R4, R5, R21,			Knobs for the switches		
R22, R23, R24	10 MΩ	Metal film, 0.6W, 1%	Output connector	3.5 mm Jack, chassis	
R6	9.1kΩ	Metal film, 0.25W, 1%	Power supply connector	Panel Mount, plug 2-pole, 6.3mm	
R7	150kΩ	Metal film, 0.25W, 1%			